JAIST Repository
https://dspace.jaist.ac.jp/

Title	Extraordinary wavelength dispersion of birefringence in cellulose triacetate film with anisotropic nanopores
Author(s)	Nobukawa, Shogo; Shimada, Hikaru; Aoki, Yoshihiko; Miyagawa, Azusa; Doan, Vu Ahn; Yoshimura, Hiroshi; Tachikawa, Yutaka; Yamaguchi, Masayuki
Citation	Polymer, 55(15): 3247-3253
Issue Date	2014-05-22
Type	Journal Article
Text version	author
URL	http://hdl.handle.net/10119/13504
Rights	Copyright (C)2014, Elsevier. Licensed under the Creative Commons Attribution-NonCommercial-NoDerivatives 4.0 International license (CC BY-NC-ND 4.0). [http://creativecommons.org/licenses/by-nc-nd/4.0/] NOTICE: This is the author's version of a work accepted for publication by Elsevier. Shogo Nobukawa, Hikaru Shimada, Yoshihiko Aoki, Azusa Miyagawa, Vu Ahn Doan, Hiroshi Yoshimura, Yutaka Tachikawa, Masayuki Yamaguchi, Polymer, 55(15), 2014, 3247-3253, http://dx.doi.org/10.1016/j.polymer.2014.05.037
Description	

JAIST
JAPAN
ADVANCED INSTITUTE OF
SCIENCE AND TECHNOLOGY

Japan Advanced Institute of Science and Technology

Extraordinary wavelength dispersion of birefringence in cellulose triacetate film with anisotropic nanopores

Shogo NOBUKAWA[1*], Hikaru SHIMADA[1], Yoshihiko AOKI[1], Azusa MIYAGAWA[1], Vu Ahn DOAN[1†], Hiroshi YOSHIMURA[2], Yutaka TACHIKAWA[3], and Masayuki YAMAGUCHI[1**]

[1]*School of Materials Science, Japan Advanced Institute of Science and Technology, 1-1 Asahidai, Nomi, Ishikawa 923-1292, Japan*

[2]*DIC Corporation, Chiba Plant, 12 Yawata-kaigandori, Ichihara, Chiba 290-8585, Japan*

[3]*DIC Corporation, Central Research Laboratories, 631 Sakado, Sakura, Chiba 285-8668, Japan*

*Corresponding author:

Tel: +81-761-51-1626

School of Materials Science, Japan Advanced Institute of Science and Technology, 1-1 Asahidai, Nomi, Ishikawa 923-1292, Japan

E-mail: nobukawa@jaist.ac.jp (S. N.)

**Corresponding author:

Tel: +81-761-51-1621

School of Materials Science, Japan Advanced Institute of Science and Technology, 1-1 Asahidai, Nomi, Ishikawa 923-1292, Japan

E-mail: m_yama@jaist.ac.jp (M. Y.)

[†]Present address: Hanoi University of Science and Technology, 1 Dai Co Viet Road, Hanoi, Vietnam

ABSTRACT

We examined birefringence in a stretched film of cellulose triacetate (CTA) after extraction of an immiscible component. The CTA film plasticized by di(2-ethylhexyl) adipate (DOA), which was added as the immiscible additive, exhibited negative birefringence to the same degree as the pure CTA film. Following removal of DOA from the film by immersion into methanol, the birefringence of the blend film changed dramatically from negative to positive. Moreover, the wavelength dependence also changed from ordinary to extraordinary, in which the absolute value of birefringence increases with wavelength. Scanning electron microscope (SEM) images revealed nanoscale ellipsoidal pores in the film after the extraction, suggesting that DOA was segregated and formed ellipsoidal domains in the CTA matrix during annealing and stretching. According to an optical theory for the nanoporous structure, we found that the form birefringence contributes to control of the optical properties of the CTA film. This phenomenon could be utilized in the design of high-performance optical films, such as quarter waveplate, because sign and wavelength dispersion of birefringence can be controlled even for a single component film.

Keywords: Nano-porous structure, Cellulose triacetate, Birefringence

INTRODUCTION

Cellulose esters for use in optical films have been studied because they have favorable optical properties including transparency, thermostability, chemical resistance, and dimensional stability [1-6]. In particular, birefringence (Δn), which is defined as the difference between two refractive indices, is one of the most important properties of optical films such as retardation and protection films [6-8]. Modern high-performance display devices, e.g., three-dimensional (3D) and organic electro luminescence (EL) displays, require a quarter waveplate with well-controlled Δn and wavelength dispersion [6, 7].

For a quarter waveplate, the proportionality relationship between Δn and wavelength is important. To improve the optical properties of films, copolymerization [7, 9], blending with other polymers or with additives [10-16], and lamination [17] have to be used because the wavelength dispersion is determined only by the chemical structure of the polymers. However, these methods exhibit some problems; copolymerization reduces thermo-resistance, and polymer blending with low compatibility decreases film transparency. With lamination, the thermal expansion mismatch between polymer sheets restricts the useful temperature range.

The birefringence of polymeric materials has three components given by:

$$\Delta n = \Delta n_O + \Delta n_G + \Delta n_F \tag{1}$$

Here, Δn_O, Δn_G, and Δn_F are orientation, glassy and form birefringence, respectively. The first term pertains to the chain orientation and the second is related to the distortion of chemical structure due to an applied force. The third term is associated with anisotropic nanostructures such as ellipsoidal structures. Based on an anisotropic dielectric theory [18] for the form birefringence, Ibn-Elhaj and Schadt [19] improved the birefringence of polymer thin films by the anisotropic nano-corrugated surface pattern. Therefore, the nano-porous structure possibly modifies birefringence of the polymeric films.

Moreover, many studies investigated porous structures in polymeric films for the application for separation membranes and separators in lithium ion second cells [20-22]. In general, porous films are prepared by using a thermo-induced phase separation (TIPS) of the matrix polymers and small amount of immiscible components, which are removed by immersing the films into selective solvents. We think that the porous structure by the TIPS technique contributes to the optical anisotropy, i.e., the form birefringence in cellulose ester films.

Because Δn_G in equation (1) is negligibly small compared to other terms for the hot-stretched polymer films, the birefringence property of stretched cellulose ester films can be modified by incorporation of an anisotropic nano-structure. In this study, the optical birefringence and its wavelength dispersion of cellulose triacetate (CTA, Figure 1), used as a model polymer, was improved with anisotropic nano-pores.

[Figure 1]

In order to design nano-porous structure such as sea-island structures in CTA films, the phase separation technique can be utilized. Since CTA is a crystalline polymer that is insoluble in most solvents, such as methanol, removal of low-mass molecules (LMs) from the sea-island structure can be accomplished using the immersion method. Based on this idea, di(2-ethylhexyl) adipate (DOA, Figure 1) was used as the immiscible LM and the pores were formed from sea-island structures resulting from phase separation of the CTA/DOA blend. In order to investigate the form birefringence, effects of chain orientation, crystallinity, and moisture content on birefringence of CTA film were also discussed.

EXPERIMENTAL

Samples

The CTA used in this study was produced by the Daicel Corporation (Japan). The degree of acetylation per pyranose unit of CTA was 2.96, as determined by ^{1}H-NMR spectroscopy. The weight-average and number-average molecular weights (M_w and M_n) of CTA were 3.5×10^5 and 1.3×10^5, respectively, as determined by gel permeation chromatography (GPC, HLC-8020 Tosoh, Japan) with TSK-GEL® GMHXL compared with polystyrene standards. DOA was used as a plasticizer to prepare the domains. DOA is commercially available and was supplied by Daihachi

Chemical Industry (Japan).

CTA and CTA/DOA films were prepared using a solution-casting method; melt processing is not applicable because thermal degradation takes place near the melting point of CTA (around 300 °C). CTA and DOA in a ratio of 10/1 wt/wt were dissolved in a binary solvent of dichloromethane/methanol (9/1 vol/vol) and a 3 wt% solution was prepared. The solvent was evaporated at room temperature (RT) for 1 day at ordinary pressure and dried *in vacuo* for 1 day without controlling humidity. Since DOA is not volatile, the composition of the blend film was controlled by the ratio of components. The film thickness was 100–150 μm.

[Table 1]

Measurements

Dynamic mechanical analysis (DMA) of the sample films was performed to measure storage and loss moduli (E' and E'', respectively) at 10 Hz as a function of temperature using a tensile oscillatory rheometer (DVE-E4000, UBM, Japan) from 0 to 250 °C at a heating rate of 2 °C min^{-1}. The glass transition temperature (T_g) was estimated from a peak of E'' in the DMA data and is shown in Table 1.

A hot-stretching test for the films was carried out with a strain rate of 0.05 s^{-1} using a tensile drawing machine (DVE-3, UBM, Japan). To avoid the thermal history effect, the films were annealed

for 10 min before stretching. The drawing temperatures (T_{draw}) were adjusted to obtain the same stress levels for CTA and CTA/DOA films, as shown in Table 1. The films were immediately quenched by cold air blowing after stretching to avoid relaxation of molecular orientation.

The orientation birefringence (Δn) of the films was measured as a function of wavelength using an optical birefringence analyzer (KOBRA-WPR, Oji Scientific Instruments, Japan). The details of the optical system have been described previously [23]. Refractive indices at various wavelengths of CTA and DOA were measured by using an Abbe refractometer (DR-M2, Atago, Japan).

To remove DOA, the stretched and unstretched films were immersed in methanol for at least 8 hours and dried *in vacuo* for 1 day at RT. The complete removal of DOA from the film was confirmed by the ^{1}H-NMR spectra before/after immersion using an AVANCE III NMR 400 (Bruker Corporation, Germany). The obtained films were kept in a humidity chamber (IG420, Yamato, Japan) at 25 °C and 50% relative humidity (RH) for 1 day to avoid the effects of uncontrolled moisture on the optical properties, as previously reported [24]. The moisture content of the films was determined using a Karl Fisher moisture meter (Mitsubishi Chemical Analytec Co. Ltd, Japan).

The morphology of the films was examined using a scanning electron microscope (SEM) (S4100, Hitachi Ltd, Japan) with an acceleration voltage of 20 kV. Prior to the observation, the surfaces of the films were coated with Pt-Pd in an ion-sputter machine (E1010, Hitachi Ltd, Japan). In order to examine the sea-island structure in CTA/DOA films, a light scattering (LS) measurement

was carried out at room temperature by using a LS analyzer (DYNA-3000, Otsuka Electronics Co., Ltd., Japan). The correlation length, which reflects the morphology of CTA/DOA films, was estimated from the LS data.

The wide-angle X-ray diffraction (WAXD) pattern was measured at RT using a powder X-ray diffractometer (RINT-2500, Rigaku, Japan) by refractive mode to evaluate the crystallinity of CTA in the films. The experiments were carried out using CuKa radiation at 40 kV and 30 mA at a scanning rate of 1° min^{-1} over 2 hours (Bragg angle range from 5 to 60°).

RESULTS and DISCUSSION

Plasticization effect of DOA on dynamic mechanical property of CTA

Dynamic mechanical properties of polymeric materials represent miscibility or immiscibility of the blends. Furthermore, the properties are also an important consideration when preparing a stretched film by melt processing because the applied stress affects the chain orientation of the polymer. Figure 2 shows the temperature dependence of E' and E'' for CTA and CTA/DOA films. The glass-to-rubber transition of the blend shifted to a lower temperature and broadened compared with that of the bulk, implying that DOA acts as a plasticizer for CTA. Yamaguchi et al. [25] reported that DOA plasticizes cellulose acetate propionate (CAP), an analog of CTA. The addition of DOA was reported to decrease the T_g of CAP by 35 °C compared with only 5 °C for CTA, suggesting that the solubility of DOA and CTA is lower than that of DOA and CAP. Therefore, DOA

is possibly immiscible with CTA on the molecular level, although the blend film was transparent after solution casting.

The rubbery plateau is also observed for general uncross-linked polymers owing to chain entanglement, and the value is at least 0.1 to 1 MPa. In Figure 2, E' curves for CTA and CTA/DOA also represent the rubbery plateau beyond 200 °C. However, the plateau modulus is over 10 MPa, which is much larger than the general value. This suggests that microcrystallites of CTA act as cross-link points. Furthermore, the plateaus in both curves represent the same level, meaning that the cross-link densities of CTA are comparable in bulk and blend. If the crystallite size is not affected by the presence of DOA, the degrees of crystallinity for CTA are similar in both systems.

[Figure 2]

Orientation birefringence of CTA and CTA/DOA

Solution-cast films of CTA and CTA/DOA were uniaxially stretched with a draw ratio of 1.5 at T_{draw}, as shown in Table 1. Stress–strain curves were obtained during stretching, as shown in Figure 3. The figure demonstrates the same stress level for the two stretched films, indicating that the chain orientations of CTA in bulk and blend are similar, as discussed later.

[Figure 3]

When polymeric materials are uniaxially stretched beyond T_g, birefringence (Δn) is generated owing to the chain orientation, as represented by:

$$\Delta n = \Delta n^0 F \tag{2}$$

Here, Δn^0 is the intrinsic birefringence reflecting the polarizability anisotropy of the chain segment for the polymers, and F is the orientation function representing the chain alignment to the stretching direction. Since stress (σ), as well as birefringence, is generated, the following relationship is obtained:

$$\Delta n = C\sigma \tag{3}$$

Here, C is a stress-optical coefficient, which is related to the polarizability anisotropy of the polymer chain. This equation is known as the stress-optical rule (SOR). From equations (2) and (3), the result in Figure 2 suggests that the chain orientation of CTA is the same in bulk and blend.

For polymer/small molecule blends, Δn is the sum of two components, as given by:

$$\Delta n = \phi_{poly}\Delta n_{poly} + (1-\phi_{poly})\Delta n_{LM} \tag{4}$$

where ϕ_{poly} is the volume fraction of the polymer, and Δn_{poly} and Δn_{LM} are the birefringence values of the two components in the pure state. However, the dynamic mechanical data in Figure 2 indicate that CTA is not completely miscible with DOA; that is, phase separation occurs. Since the CTA/DOA film seems to be transparent, the separated domain of DOA might be smaller than wavelength of visible lights (at least 400 nm), which is related to the Mie scattering. Therefore, the form birefringence (Δn_F) caused by the separated domain should be considered, as represented by:

$$\Delta n = \phi'_{CTA}\,\Delta n_{CTA} + (1-\phi'_{CTA})\Delta n_{DOA} + \Delta n_F \tag{5}$$

The prime mark in ϕ'_{CTA} represents the separated CTA-rich phase in the blend system. Figure 4 shows the wavelength dependence of orientation birefringence (Δn) of CTA and CTA/DOA films after stretching. As seen in the figure, Δn data for the two films are comparably negative, and both curves exhibit ordinary wavelength dependence, that is, the absolute value decreases with wavelength increasing. The result means that the second and third terms on the right-hand side of equation (5) are negligibly small. The form birefringence Δn_F is observed in phase-separated systems composed of two or three phases having different refractive indices. Actually, since the refractive indices (n) of CTA and DOA are almost similar (1.48 and 1.44 at 589 nm, respectively), Δn_F can be negligible as explained later.

[Figure 4]

Abd Manaf et al. [14] found that the addition of tricresyl phosphate (TCP) changed the Δn of CTA from negative to positive because the orientation of TCP was affected by intermolecular nematic interaction (NI) with the matrix polymer. Using their birefringence data from polymer/aromatic molecule blends, Nobukawa et al. [15, 16] reported that the rigid and anisotropic structure of the LM enhances the NI strength. As shown in Figure 4, the second term, $(1-\phi'_{CTA})\Delta n_{DOA}$, which is originated from DOA, is small. There are two possible explanations for this. The first possibility, from the above discussion, is the absence of NI between CTA and DOA, that is, the orientation of DOA is almost zero. The second possible influence is that the CTA matrix phase does not contain DOA because of phase separation as discuss below.

Phase separation in stretched CTA/DOA film

In order to investigate the phase separation in stretched CTA/DOA film, a static light scattering (LS) experiment was performed at room temperature. According to the statistical approaches by Debye and Bueche [26], the scattered intensity of depolarized light, I, is given as a function of scattered vector q and the correlation length ξ,

$$I = \frac{A}{\left(1+\xi^2 q^2\right)^2} \tag{6}$$

Here, A is a constant depending on the incident light. The Debye-Bueche (DB) type plots ($I^{-1/2}$ vs. q^2) represents a linear relation [27] as,

$$I^{-1/2} = \frac{1}{A^{1/2}} + \frac{\xi^2}{A^{1/2}} q^2 \tag{7}$$

Figure 5(A) shows the DB plot for CTA/DOA film after stretching, which indicates the sea-island type phase separation. By applying equation (7), the correlation length ξ was estimated to be 0.61 $\pm$0.08 μm representing the distance between the separated islands of DOA.

[Figure 5]

Birefringence and porous structure in CTA/DOA film after extraction of DOA

The stretched CTA/DOA film was immersed into methanol for a half day and dried in *vacuo*, to remove DOA from the separated islands. As a control, CTA films were also immersed. The ^{1}H-NMR spectra, which are shown in supporting information, indicated the complete extraction of DOA after the immersion. Figure 4 also shows the wavelength dispersion of Δn for CTA and CTA/DOA after immersion. The change in Δn for CTA was zero within experimental error, meaning that the chain orientation of CTA did not relax and the degree of crystallinity was held even after

immersion. In contrast, the Δn of CTA/DOA dramatically changed from negative to positive after removal of DOA. Since nanoscale DOA domains existed in the CTA/DOA before immersion, nanoscale pores might appear. The LS data of CTA/DOA film after the extraction, which is shown in Figure 5(B), exhibits the similar ξ (=0.63±0.13 μm) to the film before extraction, suggesting that the nano pores are still maintained in CTA film. In order to investigate the morphology of the film, images were taken using scanning electron microscopy (SEM).

Figure 6 compares the SEM images for unstretched, annealed and stretched CTA/DOA films after immersion. The unstretched film before annealing shown in Figure 6(A) was not subject to phase separation because no structures such as pores were observed in the surface or cross-section. In Figure 6(B), pores are visible in the cross-section of the unstretched films following the extraction. After stretching, ellipsoidal pores appeared, as shown in Figure 6(C). By assuming the affine deformation, the aspect ratio of DOA domain should be 1.5/0.8 (long axis/short axis), which is consistent with that of the ellipsoidal pore in Figure 6(C). Therefore, the SEM images suggest that DOA domains appear because of annealing above T_g, and the spherical domains are deformed into needle shapes by stretching.

[Figure 6]

Effects of moisture and crystallinity on birefringence

The effects of moisture and crystallinity on total birefringence of CTA film were confirmed as below. Abd Manaf et al. [24] investigated the effect of moisture on the Δn of CTA by controlling the humidity. According to them, 1 wt% water content increases the Δn of CTA by -2×10^{-4}. As seen in Table 2, the water contents in CTA and CTA/DOA films do not change after the immersion in methanol. Hence, the moisture effect is negligible for Δn change, as shown in Figure 4.

In general, crystalline and amorphous regions in crystalline and semi-crystalline polymers, including CTA, contribute to orientation birefringence, as represented by the following equation:

$$\Delta n = x_c \Delta n_c^0 F_c + (1 - x_c) \Delta n_a^0 F_a \tag{8}$$

Here, x_c is the degree of crystallinity. The subscripts c and a represent crystalline and amorphous regions, respectively. For generally crystalline polymers, such as poly(ethylene 2,6-naphthalate), the two intrinsic birefringences, $\Delta n_c{}^0$ and $\Delta n_a{}^0$, are not the same [28]. Therefore, the degree of crystallinity changes the total birefringence.

Figure 7 shows the X-ray diffraction (XRD) patterns for CTA and CTA/DOA films scanned under various conditions. The unstretched films for both systems showed broad peaks, which agrees with data reported by Cao et al. [29]. However, stretched and immersed films showed strong peaks reflecting crystalline structure and implying that the crystallization was induced by the hot stretching. According to equation (6), the Δn of CTA should be discussed by considering the two components from crystalline and amorphous regions. However, since the XRD patterns for

stretched and immersed films were similar, the degree of crystallinity was not changed by the stretching process. Hence, the effects of crystallinity and moisture content on Δn can be ignored.

[Figure 7]

What is the reason for the birefringence change? As represented by equation (5), the form birefringence (Δn_F) can be found in separate phases with very different refractive indices (n's). Moreover, since the porous structure that appeared after the extraction of DOA is filled with air, the difference in refractive index is much larger than that between CTA and DOA. Based on this idea, the form birefringence observed in CTA/DOA films is discussed in the next section.

Form birefringence in anisotropic porous CTA.

As can be seen in Figure 6(C), the stretched CTA/DOA film after the extraction of DOA had an anisotropic porous structure. Figure 8 is a simplified depiction of the anisotropic porous structure of the stretched CTA blend film after removal of DOA by the extraction method. Definitions of D and f are represented in the figure.

[Figure 8]

Ibn-Elhaj and Schadt [19] examined the contribution of anisotropic nano-corrugated pattern to the optical birefringence of thin polymeric films, based on the anisotropic dielectric theory. However, the theory was developed by utilizing a zero-order approximation where electric field and displacement vector are constant [30]. Therefore, Richter et al. [31] determined the form birefringence (Δn_F) in the grating system with anisotropic microstructures by applying more precise second-order solution given by,

$$\Delta n_F = n_{2,//} - n_{2,\perp} \tag{9}$$

$$n_{0,//} = \left[(1-f)n_{poly}^2 + f n_{dm}^2\right]^{1/2}$$
$$n_{0,\perp} = \left[\frac{n^2 n_0^2}{(1-f)n_{poly}^2 + f n_{dm}^2}\right]^{1/2} \tag{10}$$

$$n_{2,//} = \left[n_{0,//}^2 + \frac{1}{3}\left(\frac{D}{\lambda}\right)^2 \pi^2 f^2 (1-f^2)(n_{poly}^2 - n_{dm}^2)^2\right]^{1/2}$$
$$n_{2,\perp} = \left[n_{0,\perp}^2 + \frac{1}{3}\left(\frac{D}{\lambda}\right)^2 \pi^2 f^2 (1-f^2)\left(\frac{1}{n_{poly}^2} - \frac{1}{n_{dm}^2}\right)^2 n_{0,//}^6 n_{0,\perp}^2\right]^{1/2} \tag{11}$$

Here, the number in subscript following n represents the approximation order for the equation solution, and λ is the light wavelength. The refractive indices of polymer and pore (or domain) are denoted by n_{poly} and n_{dm}, respectively.

From equations (9)–(11), the third term in equation (5) can be calculated for CTA/DOA (before extraction) and porous CTA (after extraction) films. To fit the calculated result to the

experimental data for CTA/pore film in Figure 4, f was determined to be 0.005, and D was 0.6 μm as estimated from the LS data. These values seem to be consistent with the SEM image. However, f value is not consistent with the concentration of DOA (= 0.09), suggesting that the pore size will be reduced owing to the osmotic pressure difference between the CTA and methanol phases during the extraction. The calculated results are shown in Figure 9. The refractive indices at various wavelengths for CTA and DOA are shown in the figure while that for pore is 1.0. As shown in the figure, the contribution of Δn_F in CTA/DOA film is smaller than 10^{-6} while that in the CTA/pore film is 15×10^{-4}. In addition, the weaker wavelength dependence of the calculated Δn_F agrees with the change of Δn from the CTA/DOA and CTA/pore films represented in Figure 4.

[Figure 9]

We conclude that the form birefringence Δn_F, which is generated by the extraction of immiscible plasticizer, may change total birefringence of CTA film from negative to positive. Furthermore, since Δn_F and the orientation birefringence Δn_O exhibit weak and strong wavelength dependences, respectively, the total birefringence $(= \Delta n_F + \Delta n_O)$ shows extraordinary dependence.

In order to control the total birefringence of CTA/pore film, both Δn_O and Δn_F should be considered. The former can be controlled by the experimental conditions such as the stretching

ratio and temperature as reported in many papers. In contrast, the latter has not been investigated. The theory represented by equations (9)-(11) does not predict the stretching ratio dependence of Δn_F. We think that these stretching conditions will change size and aspect ratio of the pore. In the future work, the relationship between the pore size and Δn_F should be investigated by varying the preparation conditions of the nanoporous film.

Conclusions

We investigated orientation birefringence in a nanoporous film of cellulose triacetate (CTA), which was prepared from CTA/di(2-ethylhexyl) adipate (DOA) by immersion into methanol to extract DOA. Before the extraction, although the CTA/DOA film showed phase separation due to low miscibility, the orientation birefringence of CTA/DOA was negative and similar to that of CTA, implying that the DOA domains make no contribution to the birefringence. After the extraction, the birefringence of CTA became positive. Based on the results of moisture content, XRD and SEM, we think that the anisotropic porous structure of the CTA film after extraction is responsible for the birefringence change.

The form birefringence of the anisotropic microstructure was estimated according to surface gratings theory. As a result, agreement between theoretical and experimental results was achieved. We suggest that, even in films comprising a single component, the optical birefringence property can be modified by anisotropic nanopores created by the immersion method.

Acknowledgement

This work was partly supported by a Grant-in-Aid for Young Scientists B (25870268), and by a grant from the Kyoto Technoscience Center in 2013. The authors would like to thank Otsuka Electronics Co., Ltd. for the measurement of light scattering.

REFERENCES

1. Edgar KJ, Buchanan CM, Debenham JS, Rundquist PA, Seiler BD, Shelton MC, and Tindall D. *Prog. Polym. Sci.* 2001;26:1605-1688.
2. Law PW, Longdon A, and Willins GG. *Macromol. Symp.* 2004;208:293-322.
3. Ohno T and Nishio Y. *Macromolecules* 2007;40:3468-3476.
4. Maeda A and Inoue T. *Nihon Reoroji Gakkaishi* 2011;39:159-163.
5. Songsurang K, Miyagawa A, Abd Manaf ME, Phulkerd P, Nobukawa S, and Yamaguchi M. *Cellulose* 2012;20:83-96.
6. Yamaguchi M, Abd Manaf ME, Songsurang K, and Nobukawa S. *Cellulose* 2012;19:601-613.
7. Uchiyama A, Ono Y, Ikeda Y, Shuto H, and Yahata K. *Polym. J.* 2012;44:995-1008.
8. Tagaya A and Koike Y. *Polymer J.* 2012;44:306-314.
9. Tagaya A, Ohkita H, Harada T, Ishibashi K, and Koike Y. *Macromolecules* 2006;39:3019-3023.
10. Saito H and Inoue T. *J. Poly. Sci. Part-B Poly. Phys.* 1987;25:1629-1636.
11. Tagaya A, Iwata S, Kawanami E, Tsukahara H, and Koike Y. *App. Opt.* 2001;40:3677-3683.
12. Uchiyama A and Yatabe T. *Japan J. App. Phys. Part-1* 2003;42:3503-3507.
13. Rao YQ, Chen JL, and Ishikawa T. Control of Birefringence Dispersion Utilizing Nanocomposites. In: Company EK, editor. US Patent, vol. US 2007/0042137 A1. United State, 2005.
14. Abd Manaf ME, Tsuji M, Shiroyama Y, and Yamaguchi M. *Macromolecules* 2011;44:3942-3949.
15. Nobukawa S, Urakawa O, Shikata T, and Inoue T. *Macromolecules* 2010;43:6099-6105.
16. Nobukawa S, Aoki Y, Yoshimura H, Tachikawa Y, and Yamaguchi M. *J. Appl. Polym. Sci.* 2013;130:3465-3472.
17. Cho CK, Kim JD, Cho K, Park CE, Lee SW, and Ree M. *J. Adh. Sci. Tech.* 2000;14:1131-1143.
18. Flanders DC. *Appl. Phys. Lett.* 1983;42:492-494.
19. Ibn-Elhaj M and Schadt M. *Nature* 2001;410:796-799.
20. Lloyd DR, Kinzer KE, and Tseng HS. *J. Membr. Sci.* 1990;52:239-261.
21. Lloyd DR, Kim SS, and Kinzer KE. *J. Membr. Sci.* 1991;64:1-11.
22. Matsuyama H, Ohga K, Maki T, Tearamoto M, and Nakatsuka S. *J. Appl. Polym. Sci.* 2003;89:3951-3955.
23. Yamaguchi M, Okada K, Abd Manaf ME, Shiroyama Y, Iwasaki T, and Okamoto K. *Macromolecules* 2009;42:9034-9040.
24. Abd Manaf ME, Tsuji M, Nobukawa S, and Yamaguchi M. *Polymers* 2011;3:955-966.
25. Yamaguchi M, Iwasaki T, Okada K, and Okamoto K. *Acta Mater.* 2009;57:823-829.

26. Debye P and Bueche AM. *J. Appl. Phys.* 1949;20:518-525.
27. Pogodina NV, Siddiquee SK, van Egmond JW, and Winter HH. *Macromolecules* 1999;32:1167-1174.
28. Stein RS, Onogi S, Sasaguri K, and Keedy DA. *J. Appl. Phys.* 1963;34:80-89.
29. Cao SG, Shi YQ, and Chen GW. *J. Membr. Sci.* 2000;165:89-97.
30. Born M and Wolf E. Principles of optics. Chapt. 14. London: Cambridge University Press, 1999. pp. 735.
31. Richter I, Sun PC, Xu F, and Fainman Y. *Appl. Opt.* 1995;34:2421-2429.

Captions

Table 1 Glass transition and drawing temperatures (T_g and T_{draw}) for CTA and CTA/DOA films.

Table 2 Water content in stretched and immersed CTA and CTA/DOA films

Figure 1. Chemical structures of CTA and DOA.

Figure 2. Dynamic mechanical properties of unstretched CTA and CTA/DOA films.

Figure 3. Stress-strain curves for CTA and CTA/DOA films with the initial strain rate of 0.05 s^{-1} at T_{draw} shown in Table 1.

Figure 4. Wavelength dispersion of birefringence Δn for CTA and CTA/DOA stretched films after stretching and immersion into methanol. The increase of Δn for CTA after immersion is 2×10^{-4} while that for CTA/DOA is larger than 15×10^{-4}.

Figure 5. Debye-Bueche plot for CTA/DOA film (A) before extraction of DOA and (B) after extraction.

Figure 6. SEM images of CTA/DOA films after (A) solution-cast, (B) annealed, and (C) stretched. The black surface represents a viewing screen for the SEM image.

Figure 7. XRD patterns of (A) CTA and (B) CTA/DOA films unstretched, stretched, and after immersion.

Figure 8. Schematic illustration for the anisotropic nano-porous structure in CTA/pore system prepared from the stretched CTA/DOA films.

Figure 9. Simulated result of form birefringence Δn_F in CTA/DOA and CTA/pore films. The inset figures show the difference in refractive indices between CTA-DOA and CTA-pore.

Tables

Table 1 Glass transition and drawing temperatures (T_g and T_{draw}) for CTA and CTA/DOA films.

	T_g / °C	T_{draw} / °C
CTA	188	213
CTA/DOA	183	205

Table 2 Water content in stretched and immersed CTA and CTA/DOA films

	water content / wt%	
	stretched	*immersed*
CTA	1.76	1.51
CTA/DOA	1.30	1.31

Figures

(A)

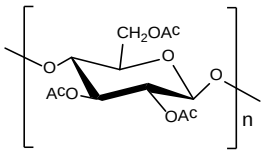

(B)

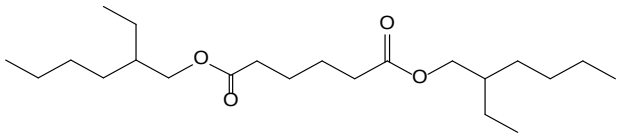

Figure 1. Chemical structures of CTA and DOA.

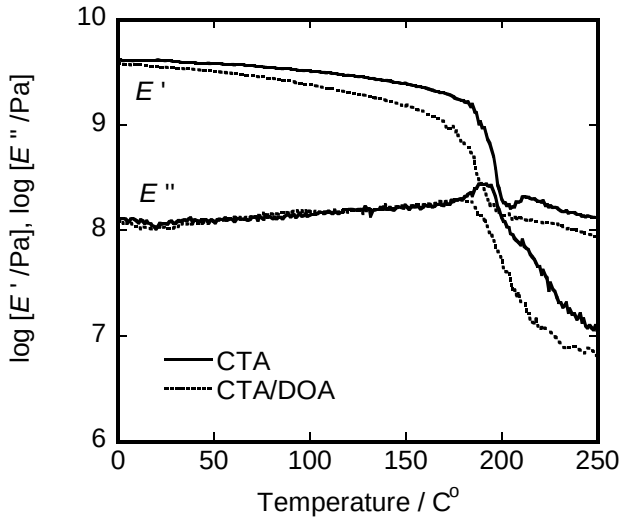

Figure 2. Dynamic mechanical properties of unstretched CTA and CTA/DOA films.

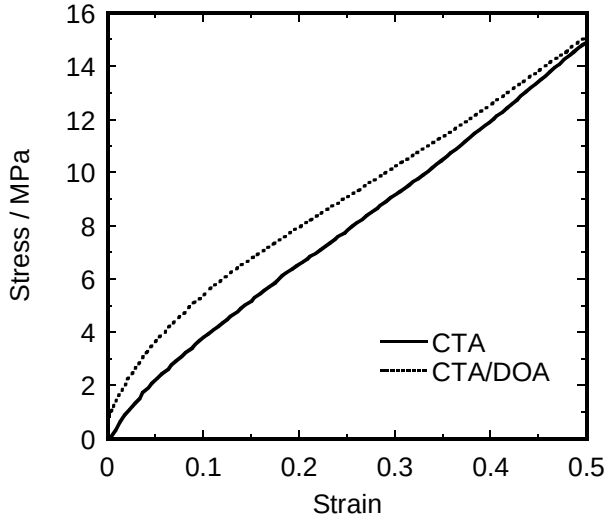

Figure 3. Stress-strain curves for CTA and CTA/DOA films with the initial strain rate of 0.05 s^{-1} at T_{draw} shown in Table 1.

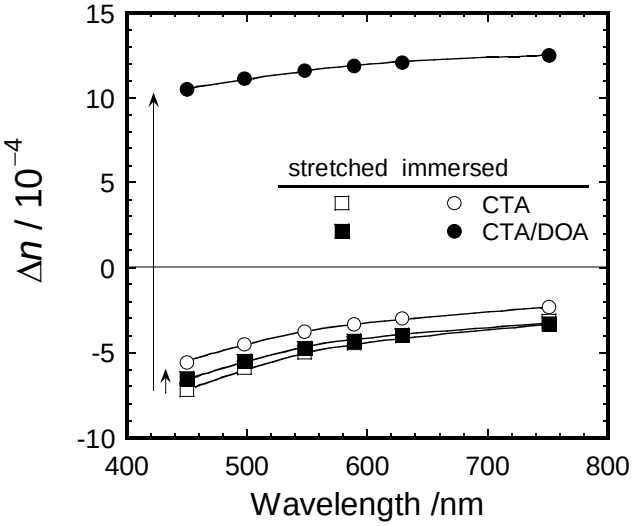

Figure 4. Wavelength dispersion of birefringence Δn for CTA and CTA/DOA films after stretching and immersion into methanol. The increase of Δn for CTA after immersion is 2×10^{-4} while that for CTA/DOA is larger than 15×10^{-4}.

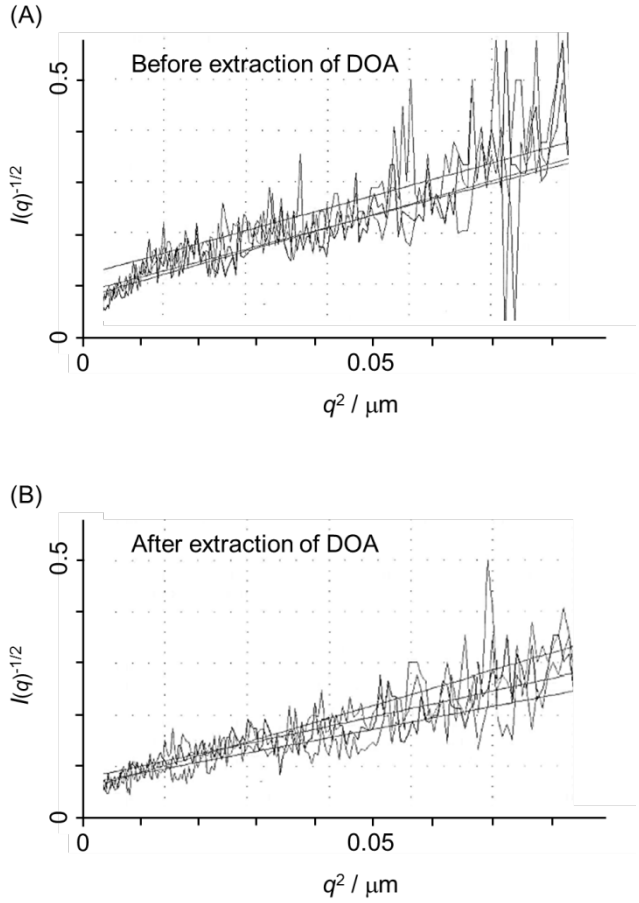

Figure 5. Debye-Bueche plot for CTA/DOA film (A) before extraction of DOA and (B) after extraction.

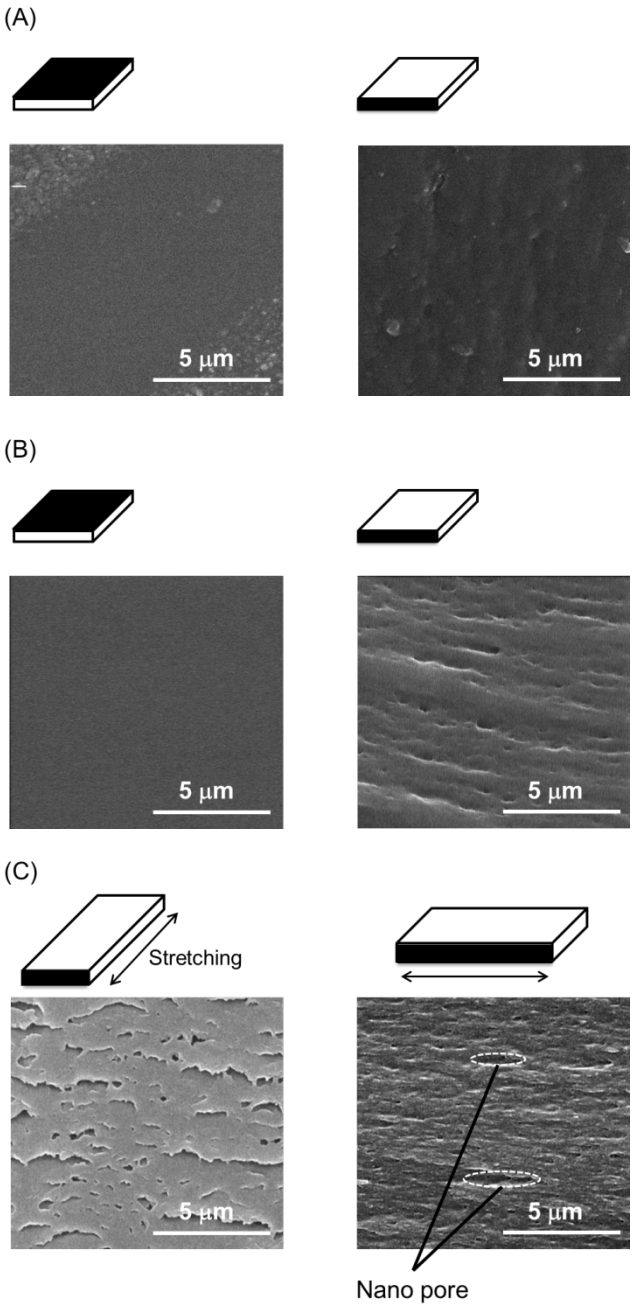

Figure 6. SEM images of CTA/DOA films after (A) solution-cast, (B) annealed, and (C) stretched. The black surface represents a viewing screen for the SEM image.

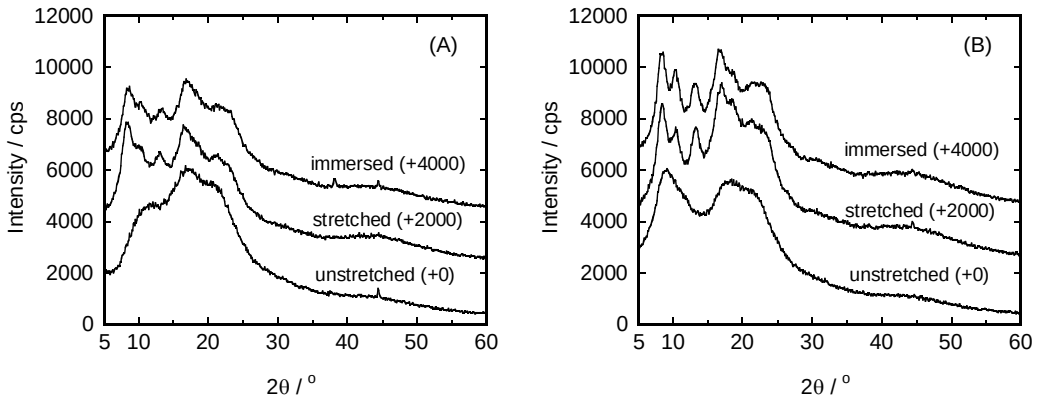

Figure 7. XRD patterns of (A) CTA and (B) CTA/DOA films unstretched, stretched, and after immersion.

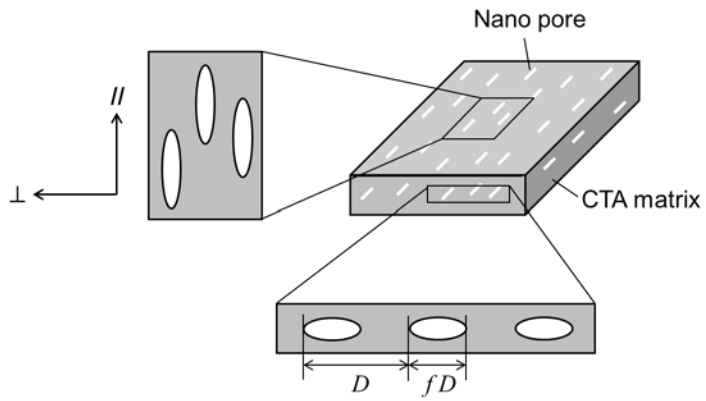

Figure 8. Schematic illustration for the anisotropic nano-porous structure in CTA/pore system prepared from the stretched CTA/DOA films.

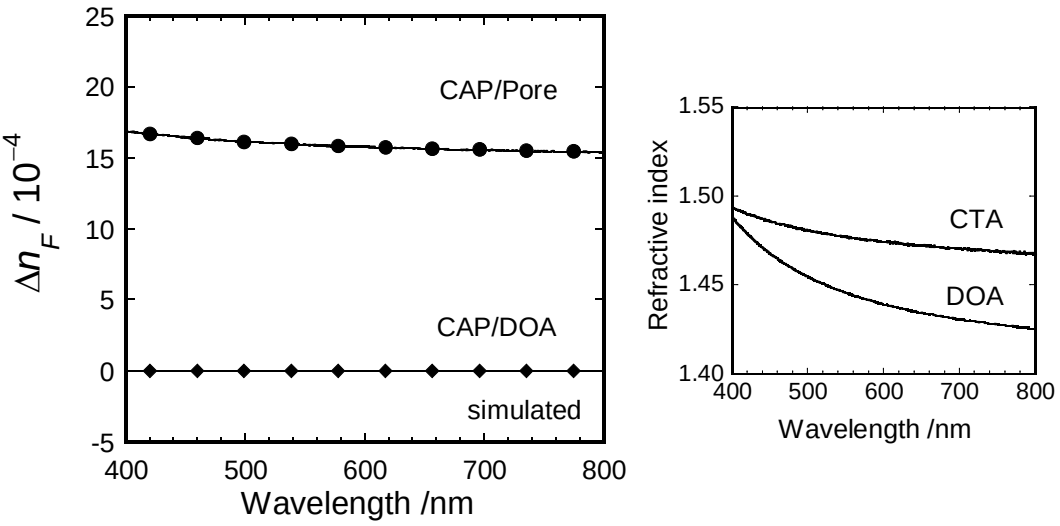

Figure 9. Simulated result of form birefringence Δn_F in CTA/DOA and CTA/pore films. The inset figure shows refractive indices of CTA and DOA at various wavelengths.

Supporting information

These figures show NMR spectra of DOA, CTA and CTA/pore after extraction of DOA. Since the spectrum of CTA/pore indicates only CTA, DOA was completely removed by the extraction method.

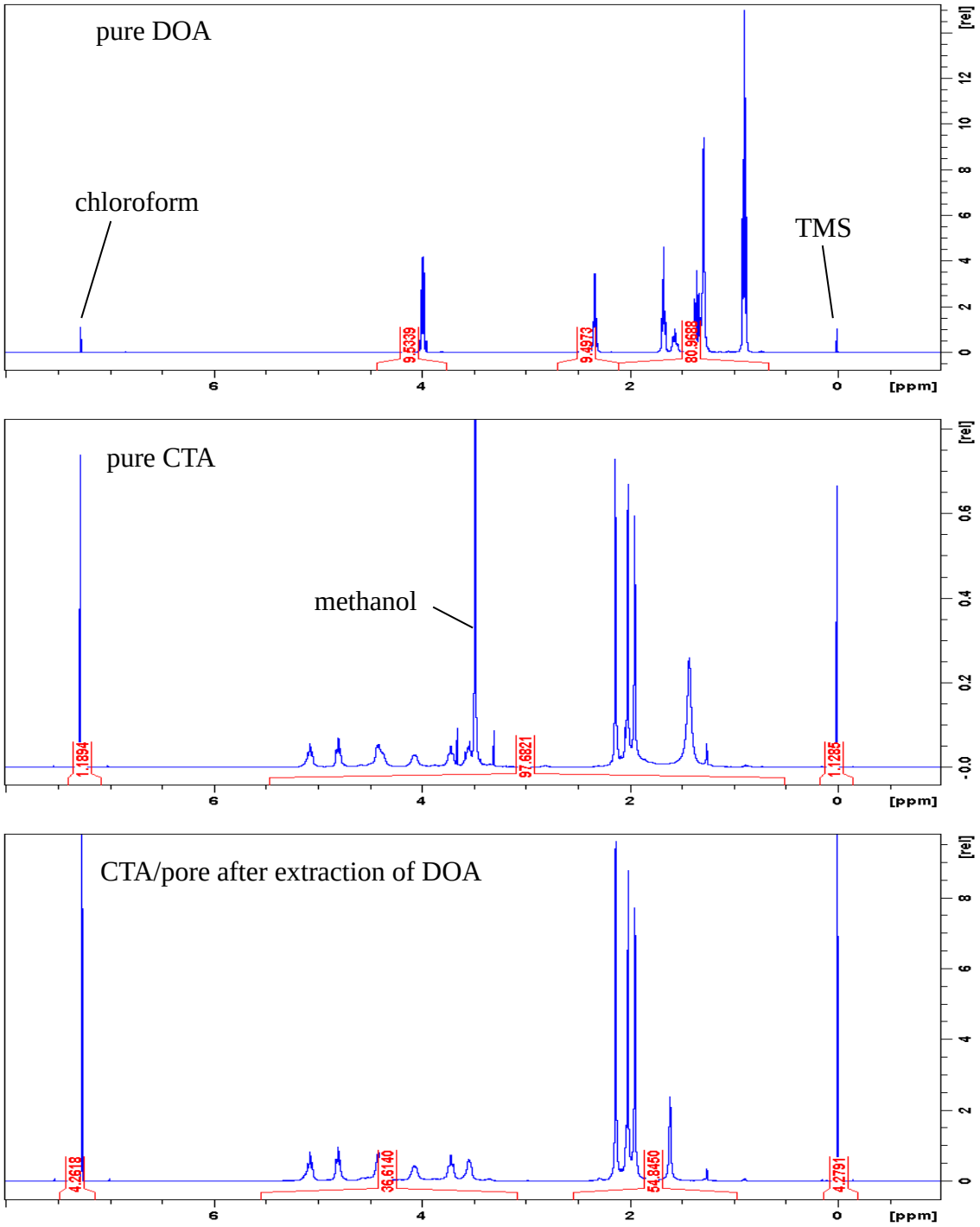

Figure S1. ^{1}H-NMR spectra of DOA, CTA and CTA/pore after extraction of DOA.